

Stable one-component quasicrystals

A. P. Smith

Department of Physics, Indiana University, Bloomington, Indiana 47405

(Received 3 December 1990)

The lowest-energy structures associated with a commonly used effective metallic pair potential are found for a wide range of values of the three parameters required by the potential. The structures tested include most of the lattices favored by the elements, the Bravais lattices with variable c/a and b/a ratios, and a number of candidate three-dimensional one-component quasicrystal structures. One of the quasicrystals is the stable structure for a region of parameter space close to the virtual-crystal parameters appropriate to the observed simple-metal quasicrystals. Energies are also evaluated for some crystalline approximants to the quasicrystals, and these structures are found to be lower in energy than the quasicrystal only for a small portion of the region of quasicrystal stability, although it is still possible that sufficiently high-order approximants are lower in energy over the entire region.

I. INTRODUCTION

It is now reasonably certain that a major contribution to the stability of the observed quasicrystalline materials comes from the electronic band-structure energy. The stoichiometry of many of the alloys appears to be governed by a Hume-Rothery rule, placing the Fermi surface near an effective Brillouin-zone boundary¹⁻³ and it has been shown through band-structure calculations for the regular crystals which approximate quasicrystals⁴ that the Fermi energy lies at or near a relative minimum in the density of electron states. There are also phenomenological models of quasicrystal stability that rely in part on the electron density and valence as parameters.⁵ However, there are no published quantitative comparisons of the band-structure energy differences between crystals and quasicrystals, in spite of the fact that a realistic estimate of energy differences would be very helpful in understanding the relative importance of different contributions to the stability.⁶ The energy comparisons that have been done^{7,8} used simple and rather arbitrary pair potentials, and the relevance of the results to the experimental systems is unclear.⁹

On the other hand, it is well known that the dependence of the electronic band-structure energy on the ionic structure can be approximated by a density-dependent effective pair potential,¹⁰⁻¹² provided that the overall density is the same for the different structures considered. This effective pair potential provides a qualitatively accurate description of the structural preferences of the simple elemental metals, and gives good quantitative agreement for the structural preferences of some of the simple metal alloys as a function of pressure and stoichiometry.^{13,14} One of the remarkable results of this approach is the wide variety of different crystal lattices that are found to minimize the energy for different values of the three parameters generally used: the ion valence Z , the volume per ion V_0 (these then determine the electron density parameter r_s through $V_0 = 4\pi Z r_s^3/3$), and the "core radius" r_c , which is the one parameter describ-

ing the pseudopotential in question. The purpose of this paper is to apply this pair potential as formulated by Hafner and Heine¹² to the question of structural energy differences between crystals and quasicrystals, to discover where we would most expect quasicrystals to form and to estimate the magnitude of potential-energy differences between the quasicrystals and the crystals that compete with them. The potential has been used in many studies on glass and liquid-metallic structures,¹⁵⁻¹⁷ but it does not seem to have been very closely examined to determine the ground states. This paper presents the lowest-energy structures among the many lattices tested, in a phase diagram similar to Fig. 14 of Ref. 12(a), and the remarkable result here is that a particular model quasicrystal is the stable structure in a region of the phase diagram that borders the region of stability for the close-packed structures.

Throughout this paper, the only quasicrystal models that we consider are those of the simple icosahedral class, with only one "acceptance domain" in the six-dimensional cubic unit cell.¹⁸ In a previous paper,¹⁹ it was found that two of the infinite number of possible acceptance domains stand out as being particularly good candidate structures, since they have relatively high sphere-packing fractions (for which the structures were first selected) and they also have Madelung constants (associated with the electrostatic energy) that approach those found for crystalline structures. These two structures, which I refer to as TSD₀ (truncated stellated dodecahedron) and RTD₀ (ruffled truncated dodecahedron) following Ref. 19 (the names are derived from the shapes of the nonconvex acceptance domains that specify the structures), are used as candidate stable quasicrystals here. It is the TSD₀ quasicrystal that is stable against all the many crystalline structures tested in the parameter-region referred to above, but there is no such region for the RTD₀ quasicrystal.

The final section of the paper will make contact with experiment by examining the region of (Z, V_0, r_c) space that is found in the "virtual-crystal" approximation from

the parameters for the elements that make up the simple-metal quasicrystalline alloys. This approximation completely ignores the chemical ordering that is in fact evident in many of these systems,^{20,21} but even so the fact that all these alloys lie very close together and lie close to the region of quasicrystal stability mentioned above suggests that the approximation catches the most important contribution to the energetic stabilization.

II. THE EFFECTIVE PAIR POTENTIAL

To second order in a local pseudopotential V_{ps} (ignoring the fact that there are nonperturbative terms associated with the formation of a crystal lattice²²) the total band-structure energy is¹⁰

$$\begin{aligned} E_{BS} &= \sum_{G (\neq 0)} [V_{ps}(G)]^2 [1/\epsilon(G) - 1] |S(G)|^2 \\ &\equiv \frac{1}{2} \sum_{G (\neq 0)} \Phi_{BS}(G) |S(G)|^2, \end{aligned} \quad (1)$$

and this expression is equally valid for a quasicrystal, if the sum over the reciprocal-lattice vectors G is replaced by a sum over the higher-dimensional reciprocal lattice, for which $S(G)$ is then an averaged geometrical structure factor^{23,24} that is a decaying function of G^\perp , the higher-dimensional complement of the reciprocal-lattice vector G . Application of the Poisson formula as appropriate for either a crystal or a quasicrystal²⁵ allows the transformation of this sum to real space (aside from the zero- q and zero- r terms that add a volume-dependent, structure-independent contribution to the total energy) to give

$$E'_{BS} = \frac{1}{2} \sum_{R_i (\neq 0)} n_i \hat{\Phi}_{BS}(R_i). \quad (2)$$

Here the factors n_i give the average frequency with which the interatomic displacement R_i is expressed in the structure. Since the direct-ion Coulomb interaction must still be accounted for, the total energy per ion associated with the ion-ion and ion-electron interactions to second order in the pseudopotential is given by

$$E = E_0(V_0) = \frac{1}{2} \sum_{R_i (\neq 0)} n_i \Phi_{\text{eff}}(R_i), \quad (3)$$

where $\Phi_{\text{eff}}(r) = \hat{\Phi}_{BS}(r) + Z^2 e^2/r$. The first term in the total energy here includes all the zero-body (electron gas) and one-body (electron-ion interaction to first order, including most of the electrostatic energy of the ion-electron system) energies, which depend on the density of the system but not on the actual positions of the ions. This structure-independent energy is so much larger than the structure-dependent part that minimizing it effectively fixes the density of the system, and in what follows it will be assumed that we compare different structures at fixed ion density.

As discovered by Hafner and Heine,¹² the most important factor in getting at least the correct sign for structural energy differences is to have a realistic and self-consistent form for the dielectric function in Eq. (1), and

then the form of the pseudopotential makes only minor changes to the structural energies. Following Ref. 12 then, we take $\epsilon(q)$ to be that described by Ichimaru and Utsumi,²⁶ and the pseudopotential to be the simple empty-core form²⁷

$$V_{ps}(q) = -4\pi Z e^2 \cos(qr_c) / q^2, \quad (4)$$

where the one parameter r_c can be obtained for a particular element from values fitted to Fermi-surface properties or liquid resistivities. The resulting real-space potential, obtained by Fourier transforming the band-structure part of Eq. (1) and adding the Coulomb part, is shown for three different sets of parameters in Figs. 1(a), 1(b), and 1(c) (the corresponding parameter values are labeled 1, 2, and 3 in Fig. 2, and are used for comparison of the energies of different structures in Table I). Note the repulsive core, the long-range Friedel oscillations, and in particular the change in the character and relative depths of the first two wells as Z and r_c change. The Fourier transform that needs to be performed in calculating this potential was accomplished here with a fast Fourier transform of the reciprocal-space function using 4096 points with a resulting real-space range of $150\pi/k_F$. Using more points or a longer range had no perceptible effect on the resulting energies.

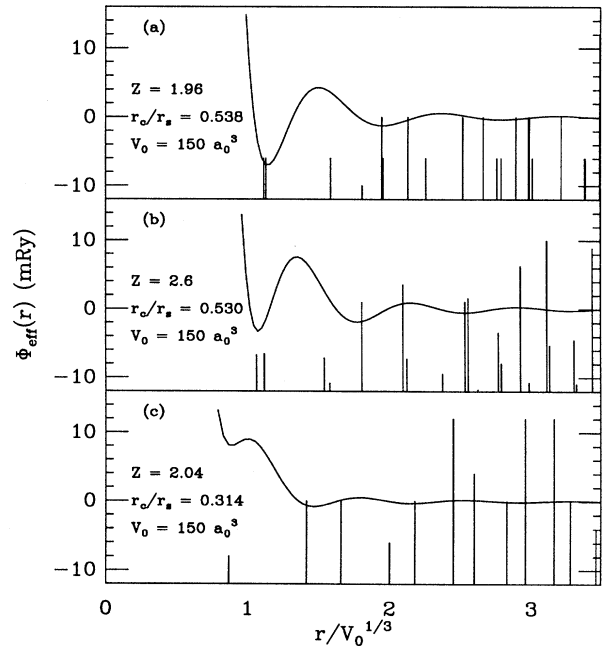


FIG. 1. The effective pair potential in real space. The sections (a), (b), and (c) are for the points 1, 2, and 3, respectively, in the phase diagram of Fig. 2. The vertical lines are the interionic distances (with heights proportional to their frequency) for the hcp lattice stable at point 1 in (a), the TSD₀ quasicrystal stable at point 2 in (b), and the diamond lattice stable at point 3 in (c).

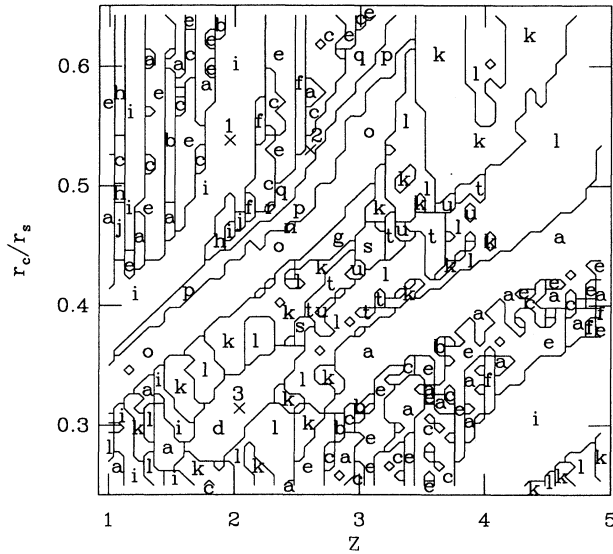


FIG. 2. The stable structures as a function of valence Z and core radius r_c (relative to r_s) at constant volume $V_0 = 150a_0^3$, (a) face-centered orthorhombic (fco), (b) body-centered cubic (bcc), (c) body-centered orthorhombic (bco), (d) diamond, (e) centered tetragonal (ct), (f) face-centered cubic (fcc), (g) α -gallium, (h) hexagonal close-packed (hcp, ideal), (i) hcp (arbitrary c/a), (j) δ -Sm (9R), (k) hexagonal, (l) base-centered orthorhombic (bsco), (n) icosahedron-based approximant at 5/3 ratio (I5/3), (o) I2/1, (p) I3/2, (q) TSD₀ quasicrystal, (r) I1/1, (s) simple cubic (sc), (t) simple tetragonal (st), and (u) simple orthorhombic (so). (a), (c), (e), (i), (k), (l), (t), and (u) are the variable lattices (for which the c/a ratios were varied to minimize the energy), while the remainder are fixed structures. The three numbered points are those covered in more detail in Fig. 1 and Table I.

III. RESULTS FOR CRYSTALS AND QUASICRYSTALS

Now that we have a real-space pair potential it is a simple matter to compare the structural energies for different crystal structures using Eq. (3), simply by tabulating the neighbor frequencies n_i out to an appropriate

cutoff distance which was here chosen to be $10V_0^{1/3}$, so that the interaction between each ion and the 4000 others nearest to it was included. Convergence in real space was checked by cutting off the sum at shorter distances, and although the absolute values of all the energies did change because of the long-range Friedel oscillations in the potential, this had the same effect on all the structures (recall that they all have the same overall density) and the energy differences appeared to have converged fairly well by a cutoff of about $4V_0^{1/3}$ (roughly 270 neighbors) but the larger cutoff was retained for the calculations just to be safe. The energies were also compared in reciprocal space, by evaluating the band-structure sum Eq. (1) and adding on the Madelung term, and aside from an overall volume-dependent shift of the energy, the energy differences between crystalline structures was the same, and in fact convergence was better for the crystals in reciprocal space than in real space. However, the quasicrystal energies had great difficulties in converging, because the six-dimensional sum involves the factor $[S(G^\perp)]^2$, which has only a $1/|G^\perp|^4$ decay at best. By altering the G^\perp cutoff, a roughly $1/G_{\max}^\perp$ convergence of the reciprocal-space band-structure energy was found, and fitting the results to that inverse-power-law function gave limiting energies in good agreement with the results of the real-space evaluation. It is because of this poor convergence of the quasicrystal sum in reciprocal space that we compare energies via real-space evaluations in the following.

The lattices tested included eight variable lattices (with b/a and c/a ratios that could be altered) and 20 fixed lattices, some of which are listed in the caption to Fig. 2, and in the case of the variable lattices the ratios were varied to minimize the energy. Many of the fixed lattices (such as for δ -Sm and α -Ga) were taken from the structures of the elements found in Ref. 28. Also among the fixed lattices tested were a number of quasicrystal approximants—regular crystals that are obtained from the six-dimensional representation of the quasicrystal by embedding the three-dimensional real space at a commensurate angle, so that the golden ratio τ is replaced by one of its Fibonacci-sequence approximations ($1/0$,

TABLE I. The energy in milliHartrees per atom from Eq. (3) (with $E_0=0$) for some of the lattices at the points marked in Fig. 2, for a volume per atom of 150 atomic units. The c/a and b/a ratios are shown in parentheses, where needed, and the asterisks mark the lowest-energy structure for each point.

Lattice	Point 1	Point 2	Point 3
fcc	-37.16	-12.73	43.69
bcc	-39.93	7.12	36.69
hcp	-46.26 (1.602)*	-5.69 (1.690)	23.34 (3.390)
hex	18.4 (0.956)	24.55 (1.055)	23.24 (1.693)
bsco	18.4 (0.957, 1.74)	24.5 (1.04, 1.70)	18.96 (0.422, 0.588)
fco	-41.1 (1.16, 1.16)	-12.74 (1.0, 0.995)	23.47 (1.866, 0.536)
diamond	227.61	201.3	11.71*
I1/1	-22.49	-13.45	42.48
I2/1	14.75	-7.07	41.45
TD3/2	-16.39	-2.88	40.49
TSD ₀	-16.29	-15.32*	42.54
RTD ₀	-11.19	-1.98	40.71

1/1, 2/1, 3/2, 5/3, . . .). Unfortunately, the acceptance domain (the unit-cell structure) must also be modified in a consistent way to preserve the local structure properties,^{29,8} and it is not known how to do this for a nonconvex domain. Therefore, the only approximants used for comparison were for the convex icosahedral domain (and also the truncated dodecahedral domain, but those were not energetically favored), so that strictly speaking the higher-order (5/3, at least) approximants could probably be improved upon by using the correct nonconvex-domain approximant crystals. The properties of the approximants used here are listed in Table II. In addition, the neighbor frequencies for the two good quasicrystals (TSD₀ and RTD₀) had previously been tabulated¹⁹ and were used here, and the neighbor frequencies for a quasicrystal with a spherical acceptance domain were also used for comparison purposes.

The results are presented in Fig. 2, showing the regions over which different phases are energetically stable, for a volume per atom of $150a_0^3$, to compare with Fig. 14 of Hafner and Heine.^{12(a)} Note in particular the region of stability of the TSD₀ quasicrystal (labeled "q") in the figure, bounded on one side (lower valence or higher r_c) by the close-packed structures and on the other by the approximants, which are followed by the α -gallium structure and other more open lattices. The general trend from close-packed to open and then to close-packed going diagonally across the diagram was noted and explained in Ref. 12. The curves (a), (b), and (c) of Fig. 1 are at the parameter values of the points labeled 1, 2, and 3 in Fig. 2, and the vertical lines in Fig. 1 indicate the interionic distances found in the optimal structure at those three points. In particular, note that the position of the first potential well for points 1 and 2 is quite similar to the close-packing distance for this density, so that in particular for point 1 the hexagonal close-packed structure (with slightly nonideal c/a) is best. For point 2, the first well is at a slightly shorter distance, and it seems the TSD₀ quasicrystal is best able to achieve that at this density. For point 3, however, the close-packing distance is very near the relative maximum in the potential, and it is optimal for the structure to have a small number of much closer neighbors, leading to stabilization of the diamond

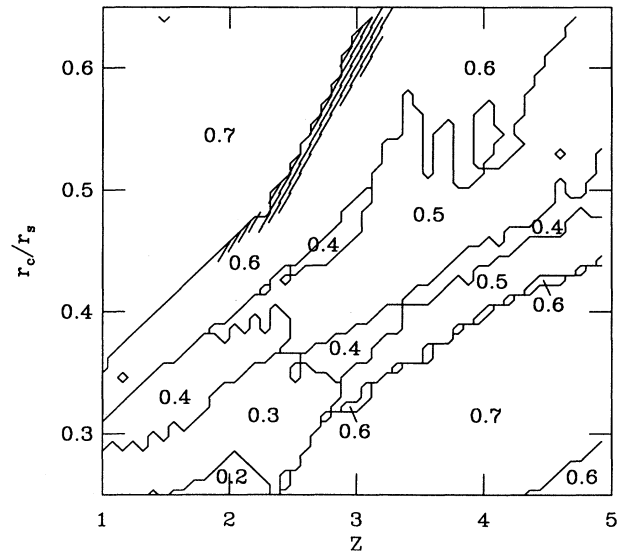


FIG. 3. The packing fractions for the structures of Fig. 2. Within each contour the packing fraction is within 0.05 of the value displayed. The quasicrystal region of Fig. 2 is shaded.

structure. Actually, the approximations here are likely to start to break down for the potential of point 3, particularly because the large value of the first minimum in the effective potential here will most likely cause the metal to expand, and the result may even be nonmetallic.

Table I lists the energies found for a selected number of the tested structures in the potentials associated with these three points in the phase diagram. We note that the energy differences between the two nearest competing low-energy structures can range from about 4 mRy (50 meV) per ion for point 2, to 14 mRy (175 meV) for point 3. It is also well known that the local approximation for the pseudopotential tends to overestimate energy differences by about a factor of 2, and so these energy magnitudes should be taken as approximate at least to that extent. In any case, the temperature associated with the difference in energy between TSD₀ and its nearest competitor (the 1/1 approximant) is roughly 500 K,

TABLE II. The nontrivial approximant crystals associated with the convex acceptance domains I_0 (an icosahedron of the ideal dimensions) and TD₀ (an ideal truncated dodecahedron) (Ref. 19). The p/q value is a rational approximation to the golden ratio $\tau [\equiv (1 + \sqrt{5})/2]$ used in the construction in the Jarić coordinate system (Ref. 29). The underlying crystal lattice is always either simple- or body-centered cubic.

Approx. polyhedron	p/q (lattice)	Basis size	Packing fraction
TD ₀	2/1 (sc)	4	0.321 135
TD ₀	3/2 (sc)	30	0.568 575
TD ₀	5/3 (bcc)	61	0.545 835
I_0	1/1 (bcc)	13	0.652 630
I_0	2/1 (sc)	93	0.551 084
I_0	3/2 (sc)	413	0.577 667
I_0	5/3 (bcc)	847	0.559 398
I_0	8/5 (sc)	7201	0.561 354

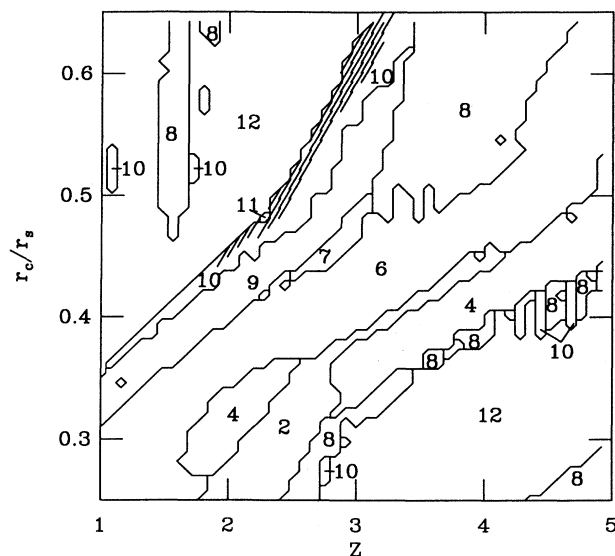


FIG. 4. The coordinations for the structures of Fig. 2. Within a contour the coordination is greater than or equal to the stated value, and here coordination is defined as the number of near neighbors no more than 15% further than the near-neighbor distance.

which is a reasonable number when compared with the temperatures at which the experimental systems transform (about 800 °C).

Figures 3 and 4 clarify the close-packed versus open division of the phase diagram by plotting contours of constant packing fraction and coordination, respectively. The packing fraction is the fraction of the volume that would be filled by nonoverlapping spheres, and is given by $\eta = \pi \rho \sigma^3 / 6$, where ρ is the ion density and σ is the near-neighbor distance. The coordination is here defined to be the average number of neighbors in a sphere of radius 1.15σ . The TSD₀ quasicrystal clearly lies right on the border of the close-packed region, with a packing fraction of 0.628 and a coordination of 10.7.

IV. VIRTUAL-CRYSTAL APPROXIMATION

Up until now the system under consideration has contained only one ionic component, characterized by the three parameters Z , r_c , and V_0 . Since the observed materials are usually alloys with at least three components, it is useful to ask what connection there may be between the apparently stable one-component quasicrystals we have found and the experimental systems. Some of the experimental systems show clear signs of chemical ordering,²⁰ but if we ignore that, then they can be crudely approximated as systems where each ion position can randomly be occupied by any one of the three different ions. The structural energy of the virtual-crystal approximation, where the system is approximated by a single ionic species with averaged valence $Z = \sum_i x_i Z_i$, and an averaged pseudopotential $V_{ps}(q) = \sum_i x_i V_{ps}(q)$, is then identical with that of the original system (there are additional energy terms that only affect the structure-independent terms in the energy) in the second-order pseudopotential perturbation theory.¹⁰ If we further assume that Vegard's law holds, the average volume per atom can be computed for any set of relative concentrations as $V_0^{1/3} = \sum_i x_i V_{0i}^{1/3}$. Furthermore, the averaged pseudopotential is reasonably well approximated by another empty-core pseudopotential, and requiring a matching of the first zero in the pseudopotential this gives an averaged core radius,

$$r_c \approx \sum_i x_i Z_i r_{ci} / Z. \quad (5)$$

In Table III the parameters calculated in this way for the combinations of elements that form *sp*-type quasicrystals are shown, and it is remarkable that all these lie close to one another in the phase diagram, although Vaks³ has claimed that they really fall into two groups according to the Hume-Rothery condition they satisfy—one for valence 2.17 and one for average valence 2.42. The phase diagram for an atomic volume of $124a_0^3$ (representative of the observed quasicrystals) is shown in Fig. 5, and we note that for this volume the region of quasicrystal stabil-

TABLE III. The valence, free-electron radius, and core radius (the last two in units of the Bohr radius $a_0 = 0.529 \text{ \AA}$) appropriate to the various *sp* elements that form quasicrystals, and the virtual-crystal parameters for several observed quasicrystals calculated from the elemental parameters. The corresponding volumes per atom are listed in the last column.

Element or alloy	Z	r_s/a_0	r_c/a_0	V_0/a_0^3
Li	1	3.26	1.06	145
Cu	1	2.67	1.24	80
Mg	2	2.65	1.39	156
Zn	2	2.30	1.27	102
Al	3	2.07	1.115	112
Ga	3	2.19	1.10	132
Al ₆₀ Li ₃₀ Cu ₁₀	2.20	2.33	1.113	117
Al _{5.5} Li _{3.3} Cu	2.12	2.37	1.112	119
Ga ₂₃ Zn ₄₀ Mg ₃₇	2.23	2.39	1.26	127
Mg ₃₇ Zn ₃₇ Al ₂₆	2.26	2.35	1.20	123
Al ₅₁ Li ₃₂ Zn ₁₇	2.19	2.36	1.13	120
Al ₅₁ Mg _{36.5} Cu _{12.5}	2.39	2.30	1.21	122
Al ₅₄ Mg ₃₇ Cu ₉	2.45	2.29	1.20	123

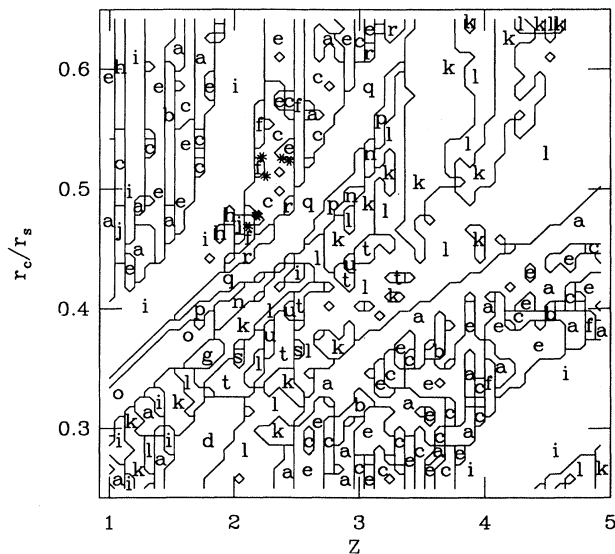


FIG. 5. The stable phases for $V_0 = 124$, using the same labels as for Fig. 2. The asterisks mark the parameters appropriate for the simple metal quasicrystals of Table III.

ity is considerably wider than for $V_0 = 150$, although the range of average valences for which the r_c/r_s range is particularly wide extends from $Z = 2.3$ to $Z = 3.2$, and so the results here do not predict a restricted range of average valences for quasicrystal stability. The location of the points of Table III is shown, and we note that they lie close to, but note quite in, the theoretical region of stability.

V. CONCLUSIONS

The density-dependent effective pair potential appropriate to the metallic state, and in particular the fixing of the density by other terms in the energy, results in a very wide range of possible structures that are stabilized for different values of the three basic parameters. Relative to the other one-component crystalline structures examined here, the TSD_0 quasicrystal appears to have no real disadvantages, in that it occupies the portion of the phase diagram that would be expected given its coordination and packing fraction. The location on the phase diagram also implies that the quasicrystals and their approximants are reasonable as metallic structures, in that they are considerably more closely packed than the distorted structures found elsewhere in the phase diagram. How-

ever, we have not compared even with all the possible Bravais lattices (there remain four that were not tried, i.e., the two monoclinic, the triclinic, and the rhombohedral structures) and in addition there are all the lattices with bases. In principle, a search over all lattices with reasonable bases (restricted to at most N points in a unit cell) could be attempted, and perhaps should be, considering the richness that has already been seen in this effective pair-potential approximation.

If a crystal *can* be found with a lower energy than the quasicrystal (and this is to be expected for at least part of the region occupied by the quasicrystal in the phase diagram here), the energy difference is likely to be of the same order as the 50 meV between the quasicrystal and the 1/1 approximant. At this level of energy difference it is clear that in a realistic model thermal effects, phonons, and other terms in the energy not considered here may still conspire to make the quasicrystal stable in spite of a disadvantage in the electronic energies.^{22,30,31} On the other hand, a prediction of stability for a quasicrystal does not mean it will necessarily be observed, since it is likely that the TSD_0 quasicrystal does not have as simple growth mechanisms as the screw dislocations found in crystals, and therefore there would be a much greater likelihood for growth into a metastable crystalline form than into the quasicrystal.

Finally, it is certainly interesting to note that the virtual-crystal approximation places many of the known quasicrystals near the quasicrystal stability region predicted here, but the crude approximations used in treating the interionic interactions in the multicomponent system do not render this a valid means of predicting the location of quasicrystals. The replacement of these approximations by pseudopotentials appropriate to the elements involved should not be terribly difficult, and should yield pair potentials that are considerably more realistic. One of the problems that remains to be worked out with the multicomponent systems is selecting multicomponent analogs of the TSD_0 acceptance domain, but considerable progress is being made in the characterization of the ordering in the experimental systems,^{21,32} and perhaps true predictions of quasicrystal formation will soon be forthcoming.

ACKNOWLEDGMENTS

The author wishes to acknowledge many useful conversations with N. W. Ashcroft and C. L. Henley. This work was supported in part by the National Science Foundation under Grants. No. DMR-87-15590 and DMR-88-02383.

¹P. A. Bancel and P. A. Heiney, Phys. Rev. B **33**, 7917 (1986).

²J. Friedel and F. Denoyer, C. R. Acad. Sci. Paris Ser. II **305**, 171 (1987).

³V. G. Vaks, V. V. Kamysenko, and G. D. Samolyuk, Phys. Lett. A **132**, 131 (1988).

⁴T. Fujiwara, Phys. Rev. B **40**, 942 (1989); T. Fujiwara and T.

Yokokawa, Phys. Rev. Lett. **66**, 333 (1991).

⁵P. Villars, J. C. Phillips, and H. C. Chen, Phys. Rev. Lett. **57**, 3085 (1986).

⁶C. L. Henley, in *Quasicrystals*, edited by T. Fujiwara and T. Ogawa, Springer Series in Solid State Sciences Vol. 93 (Springer-Verlag, Heidelberg, 1990).

- ⁷S. Narasimhan and M. V. Jarić, *Phys. Rev. Lett.* **62**, 454 (1989).
- ⁸Z. Olami, *Phys. Rev. Lett.* **65**, 2559 (1990).
- ⁹A. P. Smith and D. A. Rabson, *Phys. Rev. Lett.* **63**, 2768 (1989).
- ¹⁰W. A. Harrison, *Pseudopotentials in the Theory of Metals* (Benjamin, Reading, MA, 1966).
- ¹¹V. Heine and D. Weaire, in *Solid State Physics*, edited by H. Ehrenreich, F. Seitz, and D. Turnbull (Academic, New York, 1970), Vol. 24, p. 249.
- ¹²(a) J. Hafner and V. Heine, *J. Phys. F* **13**, 2479 (1983); (b) **16**, 1429 (1986).
- ¹³D. Stroud and N. W. Ashcroft, *J. Phys. F* **1**, 113 (1971).
- ¹⁴V. Vijayakumar *et al.*, *J. Phys. F* **16**, 831 (1986).
- ¹⁵K. Hoshino *et al.*, *J. Phys. F* **17**, 787 (1987).
- ¹⁶J. Hafner, *From Hamiltonians to Phase Diagrams* (Springer, Berlin, 1987).
- ¹⁷J. Hafner, *J. Phys. F* **14**, 2259 (1984); *Phys. Rev. Lett.* **62**, 784 (1989).
- ¹⁸P. M. deWoff, *Acta Crystallogr. Sect. A* **30**, 777 (1974); A. Janner and T. Janssen, *Phys. Rev. B* **15**, 643 (1977).
- ¹⁹A. P. Smith, *Phys. Rev. B* **42**, 1189 (1990).
- ²⁰P. Guyot and M. Audier, *Philos. Mag.* **52**, L15 (1985); V. Elser and C. L. Henley, *Phys. Rev. Lett.* **55**, 2883 (1985); C. L. Henley and V. Elser, *Philos. Mag.* **53**, L59 (1986); J. W. Cahn, D. Gratias, and B. Mozer, *J. Phys. (Paris)* **49**, 1225 (1988).
- ²¹M. de Boissieu, C. Janot, and J. M. Dubois, *J. Phys. Condens. Matter* **2**, 2499 (1990).
- ²²M. J. Kelly, *J. Phys. F* **9**, 1921 (1979).
- ²³A. P. Smith and N. W. Ashcroft, *Phys. Rev. Lett.* **59**, 1365 (1987).
- ²⁴M. V. Jarić, *Phys. Rev. B* **34**, 4685 (1986).
- ²⁵A. P. Smith and N. W. Ashcroft, *Phys. Rev. B* **38**, 12942 (1988).
- ²⁶S. Ichimaru and K. Utsumi, *Phys. Rev. B* **24**, 7385 (1981).
- ²⁷N. W. Ashcroft, *Phys. Lett.* **23**, 48 (1966).
- ²⁸R. W. G. Wyckoff, *Crystal Structures*, 2nd ed. (Interscience, New York, 1963).
- ²⁹M. V. Jarić and D. R. Nelson, *Phys. Rev. B* **37**, 4458 (1988).
- ³⁰N. W. Ashcroft, *Nuovo Cimento D* **12**, 597 (1990).
- ³¹C. L. Henley, *J. Phys. A* **21**, 1649 (1988).
- ³²S. Y. Qiu and M. V. Jarić, in *Proceedings of the Anniversary Adriatic Research Conference on Quasicrystals, Trieste, 1989* (unpublished).